J Neurophysiol 92: 3575–3581, 2004;
doi:10.1152/jn.00425.2004.

Voltage-Controlled Plasticity at GluR2-Deficient Synapses Onto Hippocampal Interneurons

Fernanda Laezza and Raymond Dingledine

Department of Pharmacology, Emory University School of Medicine, Atlanta, Georgia 30322

Submitted 26 April 2004; accepted in final form 23 August 2004

Laezza, Fernanda and Raymond Dingledine. Voltage-controlled plasticity at GluR2-deficient synapses onto hippocampal interneurons. *J Neurophysiol* 92: 3575–3581, 2004; doi:10.1152/jn.00425.2004. High-frequency stimulation of pyramidal cell inputs to developing (P9-12) hippocampal stratum radiatum interneurons expressing GluR2-lacking, Ca^{2+}-permeable AMPA receptors produces long-term depression of synaptic transmission, if *N*-methyl-D-aspartate (NMDA) receptors are blocked. Here we show that these same synapses display a remarkably versatile signal integration if postsynaptic NMDA receptors are activated. At synapses expressing GluR2-deficient AMPA receptors, tetanic stimulation that activates NMDA receptors triggered long-term potentiation or depression (LTP or LTD) depending on membrane potential. LTP was elicited at most synapses when the interneuron was held at –30 mV during the stimulus train but was typically prevented by postsynaptic hyperpolarization to –70 mV, by strong depolarization to 0 mV, by D-2-amino-5-phosphonovaleric acid, or by postsynaptic injection of the Ca^{2+} chelator bis-(*o*-aminophenoxy)-*N,N,N′,N′*-tetraacetic acid. At synapses with predominantly GluR2-containing AMPA receptors, repetitive stimulation did not change synaptic strength regardless of whether NMDA receptors were activated. The interactions among GluR2 expression, NMDA receptor expression, and membrane potential thus confer on hippocampal interneurons a distinctive means for differential decoding of high-frequency inputs, resulting in enhanced or depressed transmission depending on the functional state of the interneuron.

INTRODUCTION

The expression of distinct synaptic receptors and voltage-gated ion channels on a heterogeneous population of interneurons underlies their different integrative roles in the hippocampal circuit (Jonas et al. 2004). Long-term potentiation (LTP) and long-term depression (LTD) of excitatory synaptic strength are activity-dependent forms of synaptic plasticity triggered by Ca^{2+} entry through postsynaptic *N*-methyl-D-aspartate (NMDA) receptors (Bliss and Collingridge 1993). High-frequency afferent stimulation can depress excitatory transmission to hippocampal GABAergic interneurons (Laezza et al. 1999; Lei and McBain 2002, 2004; Maccaferri et al. 1998; McMahon and Kauer 1997). An NMDA receptor-independent LTD mechanism involves Ca^{2+} entry through postsynaptic Ca^{2+}-permeable AMPA receptors (Laezza et al. 1999; Lei and McBain 2002, 2004) and, in stratum radiatum interneurons, activation of presynaptic mGluR7 receptors (Laezza et al. 1999). High-frequency stimulation can also potentiate synaptic inputs to interneurons via an mGluR1-dependent mechanism (Perez et al. 2001) or, in other cases, by activating NMDA receptors (Christie et al. 2000). Multiple forms of interneuron synaptic plasticity add important computational versatility to the hippocampal circuit (Alle et al. 2001; Klausberger et al. 2003).

Excitatory inputs from CA3 pyramidal cells to nearby s. radiatum interneurons target postsynaptic AMPA receptors that exist in a continuum from GluR2 replete and thus relatively Ca^{2+} impermeable [producing so-called type I excitatory postsynaptic currents (EPSCs)], to GluR2-deficient, Ca^{2+}-permeable AMPA receptors (type II). Analysis of miniature EPSCs from CA3 s. radiatum interneurons showed that both type I and II EPSCs usually also express NMDA receptors with a small percentage of type II EPSCs apparently lacking NMDA receptors (McBain and Dingledine 1993).

High-frequency stimulation of pyramidal cell afferents to s. radiatum interneurons induces LTD at GluR2-deficient, but not GluR2-replete, synapses (Laezza et al. 1999). LTD occurs in the presence of NMDA receptor antagonists and is triggered by Ca^{2+} entry through AMPA receptors. Type II EPSCs are therefore both heterogeneous in terms of NMDA receptor expression and are capable of long-term changes in synaptic strength. By stratifying interneurons according to GluR2-dependent AMPA receptor properties and NMDA receptor expression, we now find that interneuron synapses expressing both NMDA receptors and Ca^{2+}-permeable AMPA receptors exhibit either LTP or LTD depending on the level of postsynaptic depolarization. In contrast, type II EPSCs lacking NMDA receptors showed exclusively LTD, whereas no change in synaptic strength after high-frequency stimulation was found at type I EPSCs expressing NMDA receptors. These results indicate that GluR2-deficient interneuron synapses can decode high-frequency signals in a bidirectional mode depending on membrane potential and postsynaptic phenotype.

METHODS

Slice preparation

Thin transverse hippocampal slices (250 μm) were prepared from neonatal (9–12 day) male Sprague-Dawley rats as previously described (Doherty and Dingledine 1997; Laezza et al. 1999). Slices were cut with a Leica Vibratome in oxygenated (95% O_2-5% CO_2), ice-cold artificial cerebrospinal fluid (ACSF) and transferred to a holding chamber at 31°C. One hour after cutting, slices were transferred to a submerged recording chamber, immobilized with a platinum frame, and continuously perfused with room temperature ACSF (composition in mM: 130 NaCl, 3.5 KCl, 1.4 $CaCl_2$ H_2O, 1.5 $MgSO_4$ H_2O, 24 $NaHCO_3$, 1.25 Na_2HPO_4, and 10 glucose).

Address for reprint requests and other correspondence: R. Dingledine, Dept. of Pharmacology, Emory University School of Medicine, 1510 Clifton Rd., Atlanta, GA 30322 (E-mail: rdingledine@pharm.emory.edu).

The costs of publication of this article were defrayed in part by the payment of page charges. The article must therefore be hereby marked "*advertisement*" in accordance with 18 U.S.C. Section 1734 solely to indicate this fact.

Recordings

Whole cell patch-clamp recordings were obtained from interneurons in the s. radiatum of the CA3 region, ≥150 μm from the CA3 pyramidal cell layer. The cell bodies were identified with infrared optics. The cell bodies were typically either fusiform or small and round for cells predominantly expressing type II EPSCs or relatively larger and polygonal for cells expressing type I EPSCs. Patch pipettes (5–7 MΩ) were prepared from borosilicate glass using a two-stage Narishige vertical puller and were filled with the following internal solution (in mM): 130 Cs-methanesulphonate, 10 HEPES, 2 $MgCl_2$, 2 MgATP, 0.3 Na_3GTP, and 0.06 spermine tetrachloride and in some cases 0.4% biocytin. When indicated, 30 mM BAPTA tetracesium salt was added to the internal solution. Internal solution was adjusted to pH 7.28 with CsOH and to 278–284 osM with H_2O. Recordings were performed using an Axopatch 1A amplifier (Axon Instruments, Union City, CA) in voltage-clamp mode. The cells were held at –70 or −80 mV throughout the recordings unless otherwise stated. Synaptic responses were typically filtered at 3 kHz using an eight-pole Bessel filter and digitized at 30 kHz on an IBM-compatible computer using pClamp8 acquisition software (Axon Instruments). Electrode capacitance compensation was achieved in cell-attached configuration in voltage-clamp mode before reaching the whole cell configuration. Compensation was performed by manually adjusting the fast mag and slow mag controls on the capacitance compensation panel of the Axonpatch 1A. This operation reduced the transient current peak response of the cell to a 10-mV voltage step by 20–50% without visually altering the kinetics of the current decay. Series resistance ($R = V$ step/I peak) was measured by applying a 1- to 5-mV voltage step filtered at 3 kHz preceding each stimulation trial. Only cells with stable series and input resistances (changes <20%) were included in this study. Monopolar platinum iridium electrodes were used to stimulate synaptic inputs arising from the CA3 pyramidal cells. The stimulating electrode was positioned in the CA3 pyramidal cell layer, and stimuli (10–100 μA) were delivered at 0.16 Hz. After a stable control baseline (5–10 min), CA3 inputs were activated at 100 Hz × 0.3 s, repeated three times at ~10-s intervals. The high-frequency stimulation was delivered while the neuron was voltage clamped at −30, 0, –70, or −80 mV. Pairing stimulation consisted of a low frequency stimulus train (1 Hz for 2 min) delivered while the postsynaptic membrane voltage was nominally clamped at −25 mV.

Drug application

Slices were perfused by the use of a peristaltic pump, at a rate of 2–3 ml/min. Drugs were added directly to the perfusion solution. Agents used were bicuculline methiodide or methochloride (10–20 μM) and D-APV (50–100 μM).

Data analysis

Synaptic current amplitudes were analyzed manually with cursors using Origin 5 or 6 software. Evoked EPSCs had a latency ranging between 1 and 5 ms, but only EPSCs occurring within a +0.5- to 1-ms window centered around the mean latency were accepted for analysis. A synaptic response was considered a failure if it occurred outside the acceptable latency for a monosynaptic connection or if its amplitude was <2 SDs of the average noise level (typically 3–4 pA). A value of 0 pA was assigned to synaptic failures. In all measurements, successes and failures were averaged together. For each cell, the effect of tetanic stimulation was measured as the mean response amplitude of all trials from 5 min after tetanus to the end of the recording, divided by the mean response over the 5 min before tetanus. A similar measurement was made in the pairing experiments. The rectification ratio (r.r.) of AMPA receptor-mediated EPSCs is defined as the ratio of synaptic chord conductances measured at +40 and −70 mV in the presence of 50–100 μM D-APV. The rectification ratio was measured at the end of each experiment. ANOVA and *t*-test were performed as appropriate to test for statistical significance.

RESULTS

NMDA receptor mediated EPSCs at excitatory synapses onto CA3 s. radiatum interneurons

We used the whole cell patch-clamp technique to record EPSCs from 56 visually identified CA3 s. radiatum interneurons in hippocampal slices of juvenile rats. EPSCs were evoked by low-intensity electrical stimulation of the nearby CA3 pyramidal cell layer in the presence of 10–20 μM bicuculline to block GABAergic inhibition. Synaptic responses with ~3-ms latency, consistent with monosynaptic connections (Wierenga and Wadman 2003), were included in this study. Synaptic responses were classified into type I or II, depending on the degree of inward rectification of their current-voltage (*I-V*) relation, measured at the end of each experiment in the presence of the NMDA receptor antagonist, 50–100 μM D-APV. For acutely isolated s. radiatum interneurons, P_{Ca}/P_{Na} rises sharply when the AMPA receptor r.r. falls <0.5, indicating a prominent contribution of Ca^{2+}-permeable AMPA receptors (Washburn et al. 1997). Likewise, when r.r. is <0.5, synaptically evoked EPSCs are especially sensitive to block by polyamine spider toxins (Laezza et al. 1999). For these reasons, we used a cutoff r.r. of 0.5 to distinguish between type I and II EPSC.

Figure 1*A* shows synaptic responses at a typical type II synapse in the presence and absence of the NMDA receptor antagonist, D-APV (100 μM), and the *I-V* relation in D-APV (Fig. 1*B*). When D-APV was omitted from the ACSF, slowly rising and decaying synaptic currents were observed at +40 mV in the majority of both type I and II EPSCs (Fig. 1, *A* and

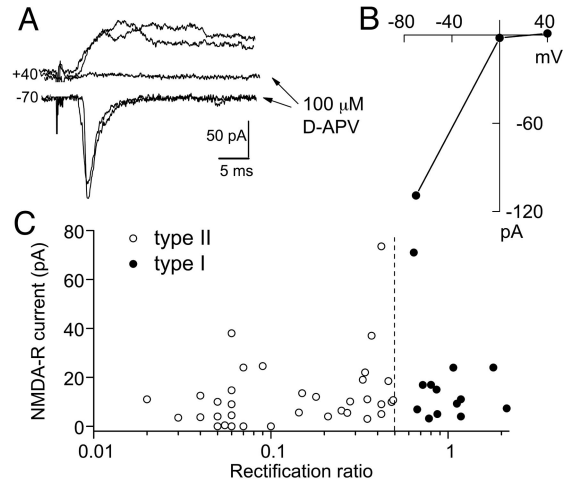

FIG. 1. Heterogeneity of *N*-methyl-D-aspartate (NMDA) receptor-mediated synaptic currents onto CA3 stratum radiatum interneurons. *A*: excitatory postsynaptic currents (EPSCs) evoked at a typical type II synapse recorded at +40 mV (*top 3 traces*) and at −70 mV (*bottom 2 traces*). D-2-amino-5-phosphonovaleric acid (D-APV; 100 μM) was present in the 2 traces indicated (←). *B*: the current-voltage relationship in D-APV of cell displayed in *A* is shown. *C*: the amplitude of NMDA receptor-mediated EPSCs is plotted against rectification ratio determined subsequently in D-APV. The amplitude of the NMDA receptor component was measured at +40 mV at a fixed latency after the stimulus (~7–9 ms after stimulus artifact). EPSC amplitudes are the average of ~50 traces in each cell. Note that 4 or 5 type II EPSCs lack a detectable NMDA receptor component.

C). However, as shown in the summary plot of 48 neurons recorded in the absence of D-APV (Fig. 1*C*), a small proportion of type II EPSCs (4 of 35) appeared to lack NMDA receptor-mediated current at +40 mV, confirming previous observation on miniature EPSCs recorded from the same population of interneurons (McBain and Dingledine 1993). These results suggest that type II EPSCs are heterogeneous in NMDA receptor expression.

Voltage-dependent plasticity at type II EPSCs

Based on the preceding results, we postulated that high-frequency stimulation at type II EPSCs might induce Ca^{2+} influx through both AMPA and NMDA receptors sufficient to induce long-term plasticity. To test this hypothesis, we used high-frequency trains (300-ms trains of 100 Hz, repeated 3 times at 10-s interval) to electrically stimulate the CA3 pyramidal cell layer in the presence of 10–20 μM bicuculline after a period of ~5 min of low-frequency (0.16 Hz) control stimulation. A short control period was used to minimize possible washout of essential cytoplasmic factors (Madison et al. 1991). We postulated that Ca^{2+} influx through NMDA receptors would predominate at –30 mV due to diminished driving force through AMPA receptors coupled with relief of Mg^{2+} block of NMDA receptors (Burnashev et al. 1995). As shown in Fig. 2*A,* high-frequency activation of type II EPSCs on interneurons voltage clamped at −30 mV increased the synaptic efficacy for ≥20 min in the absence of D-APV. This effect is designated "LTP" for simplicity, although the maximum duration of LTP was not explored. With low-intensity stimulation that evoked mainly unitary EPSCs, the synaptic failure rate was significantly decreased from mean of 42–29% after LTP ($n = 7$, $P < 0.05$, paired *t*-test), similar to previous findings for LTP in pyramidal cells (Liao et al. 1995). Seven of 10 type II EPSCs expressing functional synaptic NMDA receptors responded with synaptic potentiation lasting ≥20 min (Fig. 2*A* shows the mean responses of all 10). Evoked responses of one interneuron are shown in the *inset* to Fig. 2, *A* and *B.* The rapid appearance of posttetanic potentiation, which is typically induced by high-frequency stimulation of excitatory inputs onto pyramidal cells (Bliss and Collingridge 1993), was not observed at type II EPSCs. Rather, EPSC amplitude grew slowly over a period of 5–10 min after the tetanus (Fig. 2*A*), similar to LTD triggered by Ca^{2+}-permeable AMPA receptors (Laezza et al. 1999). Bath application of D-APV prevented LTP, as shown in Fig. 2, *C* and *D,* suggesting that NMDA receptors are necessary for LTP at type II EPSCs.

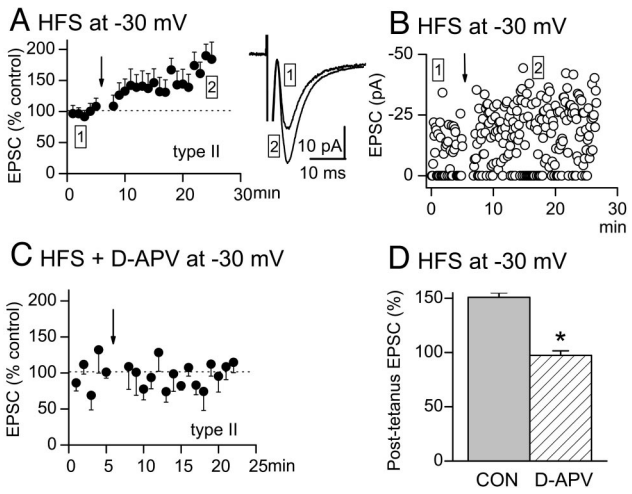

FIG. 2. NMDA receptor activation induces long-term potentiation (LTP) at GluR2-deficient synapses. *A*: type II EPSCs expressing synaptic NMDA receptors were activated by brief tetanic trains (HFS, at ↓) during voltage clamp at −30 mV. Peak EPSC amplitudes before and after the tetanic stimulus train were measured at –70 mV. Each point shows mean + SE of EPSC amplitude ($n = 10$). In 7 of these 10 experiments, tetanic stimulation induced LTP lasting up to the end of the recording (150 ± 4.1% of control, measured 5 min after tetanus to the end of the recording; $P < 0.0001$, 2-way ANOVA control vs. posttetanus, $n = 10$). *Inset*: the mean of 50 consecutive traces (including failures) before (1) and after (2) tetanic stimulation in 1 cell. *B*: example of LTP induced in response of HFS during voltage clamp in one s. radiatum interneuron. *C*: HFS delivered during voltage clamp at −30 mV in the continuous presence of 100 μM D-APV prevents LTP at type II EPSCs. Peak EPSC amplitudes before and after the tetanic stimulus train were measured at –70 mV. Each point shows mean + SE of EPSC amplitude ($n = 4$). *D*: experiments from *A* and *C* are shown as mean percentage of posttetanic EPSC amplitude in control (□) and in the presence of 100 μM D-APV (▨). (*$P < 0.0001$, unpaired *t*-test, $n = 4$).

LTD could also be evoked by stimulating a small number of synapses as shown in Fig. 3*C.* Synaptic failure rate increased from mean 46 to 86% during NMDA-receptor dependent LTD (*z* test, $P < 0.05$, $n = 3$) as observed previously for LTD caused by Ca^{2+} entry through AMPA receptor channels in the absence of NMDA receptor activation (Laezza et al. 1999). As for LTP, LTD at these synapses also began gradually after the tetanus, reaching a steady state within several minutes, and LTD was blocked by 50–100 μM D-APV (Fig. 3, *D* and *E*). These results taken together show that long-lasting modifications of synaptic strength dependent on NMDA receptor activation can occur at type II EPSCs and that the level of postsynaptic depolarization sets the direction of plasticity through activation of postsynaptic NMDA receptors.

The heterogeneity of responses at 0 mV (bar graph in Fig. 3*A*) cannot be explained by differential expression levels of Ca^{2+}-permeable AMPA receptors, as judged by the rectification ratio, but might reflect different degrees of NMDA receptor activation or Ca^{2+} buffering. Tetanic stimulation induced a slow, D-APV-sensitive summating inward current in many interneurons expressing either type II or type I EPSCs (Fig. 4, *A* and *B*). The summary data shown in Fig. 4*C* suggest that a minimum postsynaptic charge transfer during the tetanic train might be necessary for NMDA receptor-dependent LTP at type II EPSCs. Type I EPSCs could exhibit large inward train currents without plasticity (Fig. 4*C,* △). The single type II EPSC undergoing LTP after HFS at 0 mV (*cell 6* in Fig. 3*A*)

In CA1 pyramidal cells the occurrence of LTP or LTD appears to be controlled by the level of calcium influx reached during high-frequency stimulation (Lisman 1989). We hypothesized that reducing the driving force for Ca^{2+} flux through both AMPA and NMDA receptors would block LTP or convert it into LTD. To test this hypothesis, we applied the same high-frequency stimulation used for inducing LTP while interneurons were voltage clamped at 0 mV, which should decrease the driving force of Ca^{2+} flux through both AMPA and NMDA receptors (see following text, Fig. 4*C*). At 0 mV, four of six type II inputs expressing synaptic NMDA receptors underwent significant synaptic depression after tetanic stimulation as shown in the time plot, associated bar graph, and sample traces of Fig. 3, *A* and *B.* One cell (*6* in Fig. 3*A,* bar graph) showed LTP.

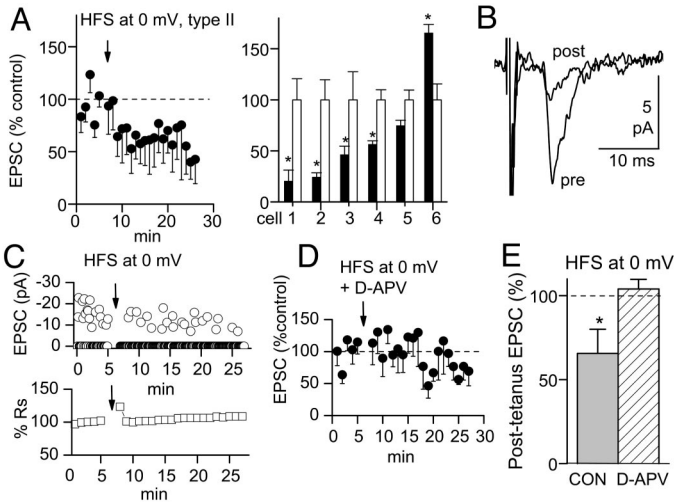

FIG. 3. NMDA receptor activation induces LTD at depolarized type II synapses. *A*: type II EPSCs expressing synaptic NMDA receptors were activated by brief tetanic trains during nominal voltage clamp to 0 mV. Peak EPSC amplitudes before and after the tetanic stimulus train were measured at –70 mV. Each point shows mean + SE of EPSC amplitude at different times before and after the stimulus train ($P < 0.0001$, 2-way ANOVA control vs. posttetanus, $n = 6$ cells). In 4 of 6 experiments, tetanic stimulation induced LTD lasting up to the end of the recording, whereas 1 cell (*6*) showed LTP under the same conditions as shown by the bar graph. □ normalized control EPSC amplitude; ■, the EPSC amplitude after the stimulus train (* $P < 0.05$, 2-way ANOVA with post hoc Bonferroni). *B*: the means of 50 consecutive traces (including failures) in 1 interneuron before (pre) and after (post) tetanic stimulation are shown. *C*: low-intensity stimulation is sufficient to induce LTD as judged by increased failure rate after the tetanus. The series resistance measurements of this cell are plotted beneath. *D*: HFS delivered during voltage clamp at 0 mV in the continuous presence of 100 μM D-APV prevents LTD at type II EPSCs. *E*: experiments from *A* and *D* are shown as mean percentage of posttetanic EPSC amplitude in the absence (▨, $n = 6$) and in the presence (▨, $n = 4$) of 100 μM D-APV. D-APV prevented depression (* $P < 0.05$, unpaired *t*-test).

had a peak inward train current greater than the other cells in that category (Fig. 4*C,* ←). The amplitude of the slow inward current elicited by HFS at 0 mV was typically smaller than that evoked at –30 mV (Fig. 3*C*) consistent with smaller driving force for cation influx.

Pairing protocol induces LTP of type II EPSCs expressing synaptic NMDA receptors

To explore the possibility that LTP observed at type II EPSCs is mediated indirectly via LTP at recurrent excitatory synapses with passive transmission to interneurons (Maccaferri and McBain 1996; Ouardouz and Lacaille 1995; Perez et al. 2001), we attempted to induce LTP at type II EPSCs using a pairing protocol. Pairing postsynaptic depolarization with low-frequency synaptic activation should induce LTP only in the cell from which EPSCs are recorded (Bains et al. 1999; Gustafson et al. 1987; Isaac et al. 1995; Liao et al. 1995; Malinow 1991; Malinow and Tsien 1990; Schuman and Madison 1994). We paired low-frequency stimulation (1 Hz) plus depolarization to −20 or −30 mV to induce LTP at four type II EPSCs expressing functional NMDA receptors, as shown in Fig. 5, *A* and *B,* and summarized in Fig. 5*C*. The failure rate of the synapse in Fig. 5*A* fell from 32 to 20% after the pairing protocol. All tested cells showed potentiation lasting ≥20 min after this protocol (Fig. 5*C*). By contrast, tetanic stimulation at –30 mV or the pairing protocol applied to the four type II EPSCs that lacked functional NMDA receptors did not produce potentiation but rather had no effect or depressed synaptic strength (Fig. 5*D*). These results demonstrate that the machinery exists to support long-lasting EPSC potentiation of type II EPSCs but only if functional NMDA receptors are present at these synapses.

Postsynaptic requirements for plasticity at type II synapses

As shown in Fig. 6*A,* synaptic NMDA receptors were also present at type I EPSCs (in all cells tested, Fig. 1*C*). If synaptic NMDA receptors are the only requirement for synaptic plasticity at excitatory inputs onto interneurons, LTP should be expressed at type I EPSCs. However, this was not the case. In Fig. 6*B,* a summary plot of six type I EPSCs expressing NMDA receptors is shown in which high-frequency stimulation was delivered at a membrane potential of –30 mV. No significant change in posttetanic EPSCs was found in any cell, regardless of whether NMDA receptors were activated at type I EPSCs during tetanic stimulation at a level comparable to type II EPSCs (Fig. 4*C,* △).

These results indicate that under our conditions NMDA receptor-mediated LTP onto s. radiatum interneurons occurs

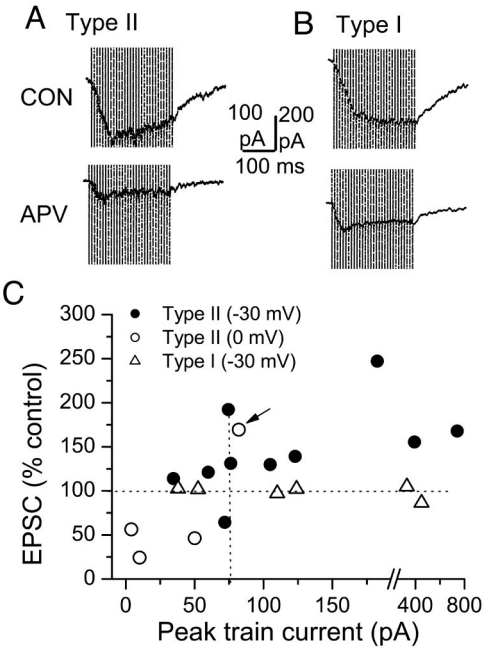

FIG. 4. Inward peak current during HFS train and plasticity at type II synapses. *A*: a slow inwared current is evoked during a train of 30 stimuli delivered over 300 ms. The shaded area reflects stimulus artifacts during the train. Averages of 3 responses to HFS of a neuron expressing type II EPSCs in the absence (*top*) or presence (*bottom*) of D-APV are shown. *B*: average of 3 responses to HFS of a neuron expressing type I EPSCs in the absence (*top*) or presence (*bottom*) of D-APV. Note the D-APV-sensitive component of the slow inward train current (summed EPSCs) during HFS in both cells. *C*: plasticity (EPSC amplitude after HFS as percent of control before HFS) is plotted against peak inward current from type II and type I EPSCs, in the absence of D-APV. Note a threshold of ~50- to 70-pA inward current during HFS for LTP induction at type II synapses. The single interneuron exhibiting LTP following HFS delivered at 0 mV (←, *cell 6* of Fig. 3*A*) had a larger inward current during the stimulus train than the other 3 cells for this condition. The amplitude of the slow inward current during HFS at 0 mV was not measured in 2 cells.

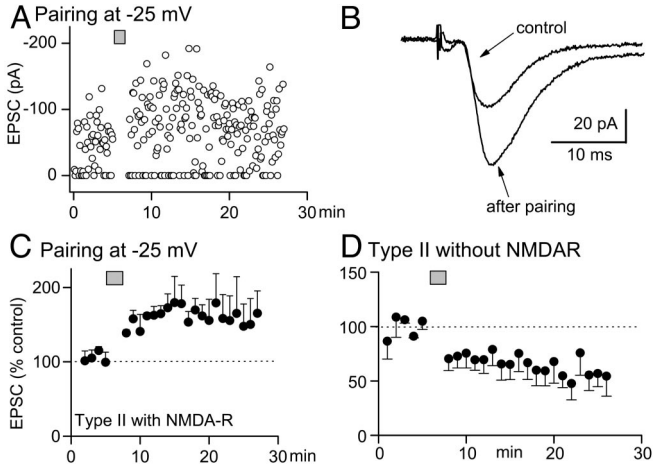

FIG. 5. Synaptic potentiation or depression of type II EPSCs by concurrent depolarization and low frequency pathway stimulation. *A*: synaptic stimulation of a type II synapse containing NMDA receptors at 1 Hz during 2-min depolarization to –25 mV induces LTP. Note that the stimulus current was high enough to activate multiple individual synaptic inputs to this interneuron. *B*: the average of 50 consecutive traces (including trials with failures) from a different interneuron before and after pairing are shown. *C*: summary of pairing-induced potentiation of type II EPSCs that express NMDA receptors (mean 160 ± 23% SE of control period, $P < 0.0001$, 2-way ANOVA comparing the control period vs. postpairing, $n = 4$). *D*: absence of potentiation in type II EPSCs lacking NMDA receptors that were subject to either the pairing protocol or tetanic stimulation at –30 mV. This condition instead depressed the EPSC ($P < 0.0001$, 2-way ANOVA, $n = 4$).

only at synapses expressing both Ca^{2+}-permeable AMPA receptors and NMDA receptors. We then tested whether chelating intracellular Ca^{2+} or hyperpolarizing the membrane potential during high-frequency stimulation could prevent LTP at type II EPSCs. Indeed, postsynaptic injection of 30 mM BAPTA into interneurons expressing type II EPSCs with NMDA receptors prevented LTP after tetanic stimulation at –30 mV ($n = 4$; Fig. 6*C*). This concentration of BAPTA effectively blocked LTD mediated by Ca^{2+}-permeable AMPA receptors at the same synapses (Laezza et al. 1999). Likewise, high-frequency stimulation with interneurons voltage clamped at −70 or −80 mV prevented LTP at six of seven type II EPSCs expressing NMDA current (Fig. 6*D*). Under these conditions, four of the seven type II EPSCs underwent synaptic depression lasting for ≥15 min (Fig. 6*D,* *, $P < 0.01$, ANOVA with post hoc Bonferroni), whereas two cells were unaffected and one potentiated. The observed depression might be caused by Ca^{2+} flux through AMPA receptors as previously shown (Laezza et al. 1999). Thus the direction of synaptic plasticity at type II EPSCs expressing NMDA receptors is exquisitely sensitive to membrane potential. No significant change in EPSC amplitude was observed at type I EPSCs after high-frequency stimulation under the same conditions ($n = 4$, $P = 0.13$, *t*-test). These results demonstrate that both postsynaptic Ca^{2+} and moderate depolarization are required for NMDA receptor-mediated LTP at GluR2-deficient synapses.

DISCUSSION

Our results demonstrate that the level of postsynaptic depolarization and the presence or absence of synaptic NMDA receptors combine to control the direction of activity-dependent changes in synaptic strength at excitatory synapses onto GABAergic interneurons of the CA3 s. radiatum that express Ca^{2+}-permeable AMPA receptors. This adds versatility to the signal integration properties of interneurons in the CA3 region. NMDA receptor-dependent LTP and LTD can occur only at type II EPSCs bearing GluR2-deficient AMPA receptors. LTP is mediated by NMDA receptors, and LTD is mediated by either AMPA or NMDA receptors, depending on membrane potential and postsynaptic glutamate receptor expression. By contrast, interneurons expressing predominantly Ca^{2+}-impermeable AMPA receptors show no forms of activity-dependent long-term plasticity under our conditions, regardless of whether NMDA receptors are present at these synapses. The capacity of s. radiatum interneurons to undergo bidirectional synaptic plasticity under our conditions is steeply dependent on the r.r. as shown by the summary in Fig. 7. Because low r.r.'s are observed for individual s. radiatum interneurons that typically express little or no GluR2 mRNA (Washburn et al. 1997), low expression of the GluR2 subunit appears to be a permissive factor for synaptic plasticity at these CA3 s. radiatum interneurons.

When type II EPSCs expressing NMDA receptors are activated at high frequency, the response at –70 mV is not uniform (Fig. 6*D*). This heterogeneity could reflect different interneuron populations, a single interneuron population in different stages of maturation, or a combination of AMPA receptor-mediated LTD countered by LTP mediated by additional Ca^{2+} entry through limited NMDA receptor activation. By contrast to type II EPSCs, CA3 s. radiatum interneurons expressing predominantly Ca^{2+}-impermeable AMPA receptors show no forms of activity-dependent long-term plasticity under our conditions, regardless of whether NMDA receptors are present at these synapses. What can account for the requirement for postsynaptic Ca^{2+}-permeable, GluR2-deficient (Geiger et al. 1995; Washburn et al. 1997) AMPA receptors that allows

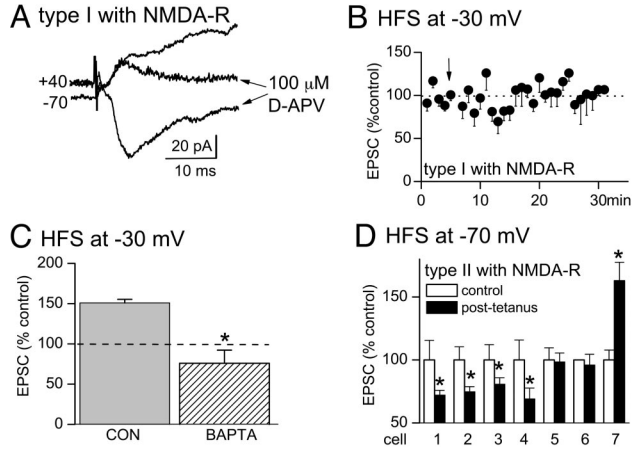

FIG. 6. Postsynaptic requirements for plasticity at CA3 inputs onto s. radiatum interneurons. *A*: type I EPSCs exhibit a D-APV sensitive slow EPSC at +40 mV (*top traces*). Traces are averages of 2–5 consecutive EPSCs. *B*: tetanic stimulation delivered to type I EPSCs while neurons are voltage clamped at −30 mV had no effect on EPSC amplitude ($n = 6$). *C*: loading interneurons expressing type II EPSCs plus NMDA receptors with 30 mM BAPTA (▨) prevents LTP induced by tetanic stimulation at –30 mV ($P < 0.01$, unpaired *t*-test, $n = 4$). *D*: type II EPSC amplitude before and after tetanus delivered at −70 or –80 mV ($n = 7$). Each pair of bars shows measurements from a single interneuron, with mean and SE of all EPSCs before (□) and after (■) the tetanus. *, $P < 0.01$ different from control, 2-way ANOVA with post hoc Bonferroni. Hyperpolarizing the interneurons blocks LTP in most interneurons.

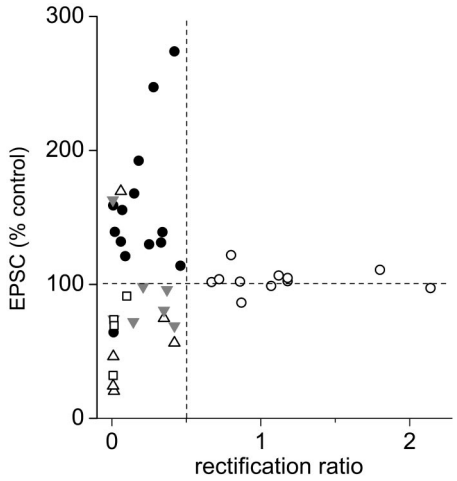

FIG. 7. Steep dependence of synaptic plasticity on postsynaptic rectification ratio. Each symbol represents a different interneuron. ○, type I under all conditions; ●, type II with NMDA receptors at –30 mV after tetanus or pairing; △, type II with NMDA receptors at 0 mV after tetanus; gray triangles: type II with NMDA receptors at –70 mV after tetanus; □, type II without NMDA receptors at –30 mV after tetanus. Vertical - - -, rectification ratio = 0.5.

NMDA receptor-mediated LTP and LTD? First, a dual route for postsynaptic Ca^{2+} influx could be involved. If both AMPA and NMDA receptors participate in LTP, Ca^{2+} entry through both receptor types might be required. If this is the case, LTP or LTD at type II EPSCs might occur depending on the total amount of Ca^{2+} fluxing through postsynaptic receptors (cf. Fig. 4*C*), similar to what has been reported in principal cells (Cummings et al. 1996). Second, AMPA receptors lacking GluR2 might associate with specific synaptic scaffolding proteins that promote cycling of AMPA receptors to the interneuron plasma membrane (Braithwaite et al. 2002; Burette et al. 1999, 2001). Likewise, GluR2-deficient synapses onto interneurons might possess uniquely specialized synaptic domains (Goldberg et al. 2003), allowing a wide range of plasticity either mediated by AMPA receptors or by AMPA and NMDA receptors. Third, interneurons expressing type II EPSCs might display large cytoplasmic Ca^{2+} transients above the threshold needed for plasticity (Cormeir et al. 2001; Cummings et al. 1996; Lisman 1989), perhaps due to insufficient Ca^{2+}-buffering mechanisms in these interneurons. Fourth, the GluR2 lacking phenotype at type II EPSCs could be linked to an intrinsic ability of the synapses to be remodeled. Finally, although there is clear evidence for a postsynaptic role, we emphasize that our observations do not rule out a contribution of heterogeneity in the presynaptic terminal to LTP and LTD. None of these possible explanations can be ruled out at present.

The ability of type II EPSCs to show LTP after the pairing protocol that failed to revealed potentiation in other interneurons (Maccaferri and McBain 1996) indicates that LTP at type II EPSCs is probably not the result of potentiation passively propagated from CA3 pyramidal neuron collaterals. Low-frequency stimulation (1 Hz) also fails to produce LTP at mossy fibers to CA3 synapses (Kobayashi et al. 1996), arguing against the possibility that LTP, seen at type II EPSCs with the pairing protocol, could have been caused by inadvertent mossy fiber stimulation. Passive propagation seems unlikely in any case because the typical latency of synaptic responses was ~3 ms with a jitter of 1–2 ms, consistent with a monosynaptic connection (Wierenga and Wadman 2003). Finally, the voltage-dependent control of plasticity, the absence of LTP at type II EPSCs lacking NMDA receptors or treated with intracellular calcium chelator, and the absence of plasticity at type I EPSCs also argue against passive propagation. If LTP that we study was a circuitry phenomenon, it would likely occur regardless of any postsynaptic condition.

The voltage range for induction, and the postsynaptic receptor requirements, thus cause the control of long-term changes of synaptic strength at type II EPSCs to be substantially different from control of excitatory inputs onto principal cells. GluR2-deficient interneuron synapses are capable of decoding high-frequency stimuli differently depending on their functional state. This property should enable GluR2-deficient synapses to be influenced in a subtle way by modulatory agents. For example, postsynaptic GABAergic inhibition in adult animals could favor LTD through Ca^{2+}-permeable AMPA receptors by selectively shunting postsynaptic NMDA receptors and by hyperpolarizing the membrane voltage (Staley and Mody 1992). Alternatively, early in development activation of postsynaptic GABAergic synapses could cause depolarization and thereby favor LTP. All recordings were done in bicuculline to eliminate GABA-A responses, but future work could investigate whether GABAergic inhibition controls the *direction* of plasticity of type II EPSCs. Activation of presynaptic $GABA_B$ receptors could add a further level of modulation of the inhibitory tone by suppressing GABA release (Mott and Lewis 1994). Similarly, activation of group III mGluRs at inhibitory terminals synapsing onto interneurons, possibly by glutamate spillover (Semyanov and Kullmann 2000), could suppress GABA release and increase postsynaptic depolarization to favor activation of NMDA receptors. The strength of GABAergic inputs to these inhibitory interneurons is likely to influence strongly the direction of synaptic plasticity in response to high-frequency input; this enriches the potential mission of GluR2-deficient interneurons in the CA3 hippocampal circuit.

ACKNOWLEDGMENTS

We thank S. Traynelis for npm52 software, G. Maccaferri for discussions, and D. Mott, J. Huettner, and C. McBain for helpful comments on the manuscript.

Present address of F. Laezza: Dept. of Anatomy and Neurobiology, Washington University, St Louis, MO 63141.

GRANTS

This work was supported by the National Institute of Neurological Disorders and Stroke (R. Dingledine) and the Epilepsy Foundation of America and Sigma XI (F. Laezza).

REFERENCES

Alle H, Jonas P, and Geiger JRP. PTP and LTP at a hippocampal mossy fiber interneuron synapse. *Proc Natl Acad Sci USA* 98: 14708–14713, 2001.

Bains JS, Longacher JM, and Staley KJ. Reciprocal interactions between CA3 network activity and strength of recurrent collateral synapses. *Nat Neurosci* 8: 720–726,1999.

Bliss TV and Collingridge GA. A synaptic model of memory: long-term potentiation in the hippocampus. *Nature*: 361: 31–39, 1993.

Braithwaite SP, Xia H, and Malenka RC. Differential roles for NSF and GRIP/ABP in AMPA receptor cycling. *Proc Natl Acad Sci USA* 99 7096–7101, 2002.

Burette A, Khatri L, Wyszynski M, Sheng M, Ziff EB, and Weinberg RJ. Differential cellular and subcellular localization of AMPA receptor-binding protein and glutamate receptor-interacting protein. *J Neurosci* 21 495–503, 2001.

Burette A, Wyszynski M, Valtschanoff JG, Sheng M, and Weinberg RJ. Characterization of glutamate receptor interacting protein-immunopositive neurons in cerebellum and cerebral cortex of the albino rat. *J Comp Neurol* 411 601–612, 1999.

Burnashev N, Zhou Z, Neher E, and Sakmann B. Fractional calcium currents through recombinant GluR channels of the NMDA, AMPA and kainate receptor subtypes. *J Physiol* 485: 403–418, 1995.

Christie BR, Franks KM, Seamans JK, Saga K, and Sejnowski TJ. Synaptic plasticity in morphologically identified CA1 stratum radiatum interneurons and giant projection cells. *Hippocampus* 10: 673–683, 2000.

Cormeir RJ, Greenwood AC, and Connor JA. Bidirectional synaptic plasticity correlated with the magnitude of dendritic calcium transients above a threshold. *J Neurophysiol* 85: 399–406, 2001.

Cummings JA, Mulkey RM, Nicoll RA, and Malenka RC. Ca^{2+} Signaling requirements for long-term depression in the hippocampus *Neuron* 16: 825–833, 1996

Doherty JJ and Dingledine R. Regulation of excitatory input to inhibitory interneurons of the dentate gyrus during hypoxia. *J Neurophysiol* 77: 393–404, 1997.

Geiger JR, Melcher T, Koh DS, Sakmann B, Seeburg PH, Jonas P, and Monyer H. Relative abundance of subunit mRNAs determines gating and Ca^{2+} permeability of AMPA receptors in principal neurons and interneurons in rat CNS. *Neuron* 15: 193–204, 1995.

Goldberg JH, Tamas G, Aronov D, and Yuste R. Calcium microdomains in aspiny dendrites. *Neuron* 40: 807–821, 2003.

Gustafsson B, Wigstrom H, Abraham WC, and Huang YY. Long-term potentiation in the hippocampus using depolarizing current pulses as the conditioning stimulus to single volley synaptic potentials. *J Neurosci* 7: 774–780, 1987.

Isaac JTR, Nicoll RA, and Malenka RC. Evidence for silent synapses: implications for the expression of LTP. *Neuron* 15: 427–434, 1995.

Jonas P, Bischofberger J, Fricker D, and Miles R. Interneuron diversity series: fast in, fast out—temporal and spatial signal processing in hippocampal interneurons. *Trends Neurosci* 27: 30–40, 2004.

Klausberger T, Magill PJ, Marton LF, Roberts JD, Cobden PM, Buzsaki G, and Somogyi PAL. Brain-state- and cell-type-specific firing of hippocampal interneurons in vivo. *Nature* 421: 844–848, 2003

Kobayashi K, Manabe T, and Takahashi T. Presynaptic long-term depression at the hippocampal mossy fiber-CA3 synapse. *Science* 273: 648–501, 1996.

Laezza F, Doherty JJ, and Dingledine R. Long-term depression in hippocampal interneurons: joint requirement for pre- and postsynaptic events. *Science* 285: 1411–1414, 1999.

Lei S and McBain CJ. Distinct NMDA receptors provide differential modes of transmission at mossy fiber-interneuron synapses *Neuron* 33: 921–933, 2002.

Lei S and McBain CJ. Two Loci of expression for long-term depression at hippocampal mossy fiber-interneuron synapses. *J Neurosci* 24: 2112–2121, 2004.

Liao D, Hessler NA, and Malinow R. Activation of postsynaptically silent synapses during pairing-induced LTP in CA1 region of hippocampal slice. *Nature* 375: 400–404, 1995.

Lisman J. A mechanism for the Hebb and the anti-Hebb processes underlying learning and memory. *Proc Natl Acad Sci USA* 86: 9574–1978, 1989.

Maccaferri G and McBain CJ. Long-term potentiation in distinct subtypes of hippocampal nonpyramidal neurons. *J Neurosci* 16: 5334–5343, 1996.

Maccaferri G, Toth K, and McBain CJ. Target-specific expression of presynaptic mossy fiber plasticity. *Science* 279: 1368–1371, 1998.

Madison DV, Malenka RC, and Nicoll RA. Mechanisms underlying long-term potentiation of synaptic transmission. *Annu Rev Neurosci* 14: 379–97, 1991.

Malinow R. Transmission between pairs of hippocampal slice neurons: quantal levels, oscillations and LTP. *Science* 252: 722–724, 1991.

Malinow R and Tsien RW. Presynaptic enhancement revealed by whole-cell recordings of long-term potentiation in rat hippocampal slices. *Nature* 346: 177–180, 1990.

McBain C and Dingledine R. Heterogeneity of synaptic glutamate receptors on CA3 stratum radiatum interneurons of rat hippocampus. *J Physiol* 462, 373–392, 1993.

McMahon LL and Kauer JA. Hippocampal interneurons express a novel form of synaptic plasticity. *Neuron* 18: 295–305, 1997.

Mott DD and Lewis DV. The pharmacology and function of central GABAB receptors. *Int Rev Neurobiol* 36: 97–223, 1994.

Ouardouz M and Lacaille JC. Mechanisms of selective long-term potentiation of excitatory synapses in stratum oriens/alveus interneurons of rat hippocampal slices. *J Neurophysiol* 73: 810–819, 1995.

Perez Y, Morin F, and Lacaille J-C. A Hebbian form of long-term potentiation dependent on mGluR1a in hippocampal inhibitory interneurons. *Proc Natl Acad Sci USA* 98: 9401–9406, 2001.

Schuman EM and Madison DV. Locally distributed synaptic potentiation in the hippocampus. *Science* 263: 532–536, 1994.

Semyanov A and Kullmann DM. Modulation of GABAergic signaling among interneurons by metabotropic glutamate receptors. *Neuron* 25 663–72, 2000.

Staley KJ and Mody I. Shunting of excitatory input to dentate gyrus granule cells by a depolarizing $GABA_A$ receptor-mediated postsynaptic conductance. *J Neurophysiol* 68: 197–212, 1992.

Washburn, MS, Numberger M, Zhang S, and Dingledine R. Differential dependence on GluR2 expression of three characteristic features of AMPA receptors. *J Neurosci* 17: 9393–9406, 1997.

Wierenga CJ and Wadman WJ. Excitatory inputs to CA1 interneurons show selective synaptic dynamics. *J Neurophysiol* 90: 811–821, 2003.